A Study on the Pumping Performance of a Molecular Drag Pump in the Rarefied Gas Flow

MYOUNG-KEUN KWON and YOUNG-KYU HWANG

School of Mechanical Engineering, Sungkyunkwan University
300 Chunchun-Dong, Jangan-Gu, Suwon city, Kyungki-Do 440-746, South Korea

Abstract. The pumping performance of a disk-type molecular drag pump (MDP) are studied for the variation of the channel depth and of the clearance between a rotor and stator by the three-dimensional direct simulation Monte Carlo (DSMC) method. The gas flow mainly belongs to the molecular transition flow region. Spiral channels of a disk-type MDP rotor are cut on both the upper and lower sides of rotating disks, but the stationary disks are planar. The rotor of the disk-type MDP is equipped with ten spiral blades. To simplify the computational model and to shorten the calculation time, only one single flow channel is calculated. The full computational domain is linked by five regions including a radial clearance area between the rotor and casing wall, two regions of spiral channels on the upper and lower sides of the rotor, an inlet region of the pumping channel, and an outlet region of the pumping channel. The flow-meter method is adopted here to calculate the pumping speed. The interaction between molecules is described by the variable hard-sphere model. The no time counter method is used as a collision sampling technique. For the calculation of the rotational energy exchange between the colliding molecules, the Borgnakke-Larsen phenomenological model is employed. As a consequence of results, both the depth of channel and the vertical clearance area between a rotor and stators have a significant effect on the pumping performance. A three-dimensional DSMC method for the analysis of steady rarefied flows in a single-stage disk-type MDP has been developed. Pressure density fields were obtained by the DSMC simulation in the rotor.

.

Keywords: Molecular drag pump, Disk-type molecular drag pump, Pumping speed, DSMC.
PACS: 07.30.Cy

INTRODUCTION

The molecular drag pump (MDP) was invented in the 1920's. It was recently reintroduced with the hybrid molecular pumps made by combining a turbomolecular pump (TMP) and a MDP, as a high-vacuum pump competing with the conventional TMP with Roots blowers.

The vacuum pumping system composed of a drag pump with a dry backing pump is widely used in the etching and high-density plasma processes. Recently, the semiconductor industry is getting into a new era by using 300 mm wafers. For example, compound and hybrid molecular pumps have gained wide attention because of their high pressure and larger throughput capabilities to provide the ultra-clean environment productivity.

The MDP is widely used, in combination with, a TMP in order to improve the pumping performance of it.[1,2] Namely, the compound or hybrid molecular pumps have gained wide attention because of their increased pumping throughput and higher discharge pressure. The MDP may be of the helical-type (Holweck) or disk-type (Siegbahn) design. Heo and Hwang[3,4] numerically studied the molecular transition and slip flows arising in the flow channels of a disk-type molecular drag pump (DTDP) by using both the direct simulation Monte Carlo method (DSMC) and the Navier-Stokes equations with slip boundary conditions.

Liu and Pang[5] studied the effect of a spiral channel on the disk of a DTDP on the pumping performance in the free molecular flow by using the matrix-probability method. Shi *et al.*[6,7] theoretically investigated the influence of geometrical parameters of a spiral channel on performance by the test particle Monte Carlo method. Sawada and Nakamura[8,9] extensively analyzed the pumping mechanism by solving the Navier-Stokes equation with slip

boundary conditions. Sawada[10] also found that the compression performance is improved by the generation of vortices in the molecular-transition regime due to the onset of turbulence in the channel.

In case of the present study, the pumping action of a DTDP is produced by the motion of a grooved rotating disk surface over a planar stationary disk, where the vertical clearance between the two is small. On impact with gas molecules, the rotating disk impulse is transmitted to molecules, thus giving them a speed component in the direction of rotation of the rotor.

Previous studies of a DTDP[11,12] have been performed for several configurations of the stationary channels on stators and of the rotating ones on rotors.[3,4] Shi *et al.* [6,7] found that the performance of the rotating channels is better than that of the stationary ones in the free molecular flow. Similarly, Heo and Hwang[11] revealed that the pumping performance of rotating channels is relatively higher in the regimes of molecular transition and slip flows because the rotating channels impart angular momentum directly to the gas molecules. Also, Heo and Hwang[12] studied the pumping characteristics of a two-stage DTDP, whose spiral channels were on the rotating disks, by the DSMC[13] method. In the published papers[15,16], the experimental results have been compared with numerical ones obtained by the DSMC method. Results of numerical study show good quantitative agreement with the experimental data.

The present study is concerned with the analysis of the molecular transition flows arising in rotating spiral channels of a single-stage DTDP by the three-dimensional DSMC method. The pumping characteristics, associated with pressure density fields, of a DTDP, whose pumping channels are cut on the rotating disk, are calculated for the variation of the vertical clearance $\triangle d$ between a rotor and stator in the range of $0.1 \leq \triangle d \leq 1.0$ mm and the radial clearance $\triangle R$ between a rotor and casing wall at $\triangle R = 1$ mm, respectively. The depth of channels d are $1 \leq d \leq 3.5$ mm. It will be shown that both the depth of channel and the vertical clearance have a significant effect on the pressure rise of a DTDP.

Numerical Method and Model

The DSMC method used in this study is based on the principles described by Bird.[13] The interaction between molecules is modeled by the variable hard sphere scattering assuming an inverse-power interatomic potential. The no time counter method is used as a collision sampling technique. For the calculation of the rotational energy exchange between the colliding molecules, the Borgnakke-Larsen phenomenological model[14] is employed. In order to limit the memory and CPU required to perform the calculations, the computational domain of the DTDP is restricted to one blade passage. In the analysis of the rotor configuration the rotating frame of reference is used.

The rotor has ten blades with an Archimedes' spiral profile, with an exit angle of 10° relative to the tangent. At the inlet, the blade angle relative to the tangent is 30°. Detail dimensions of the DTDP illustrated in Fig. 1(a) are listed in Table 1.

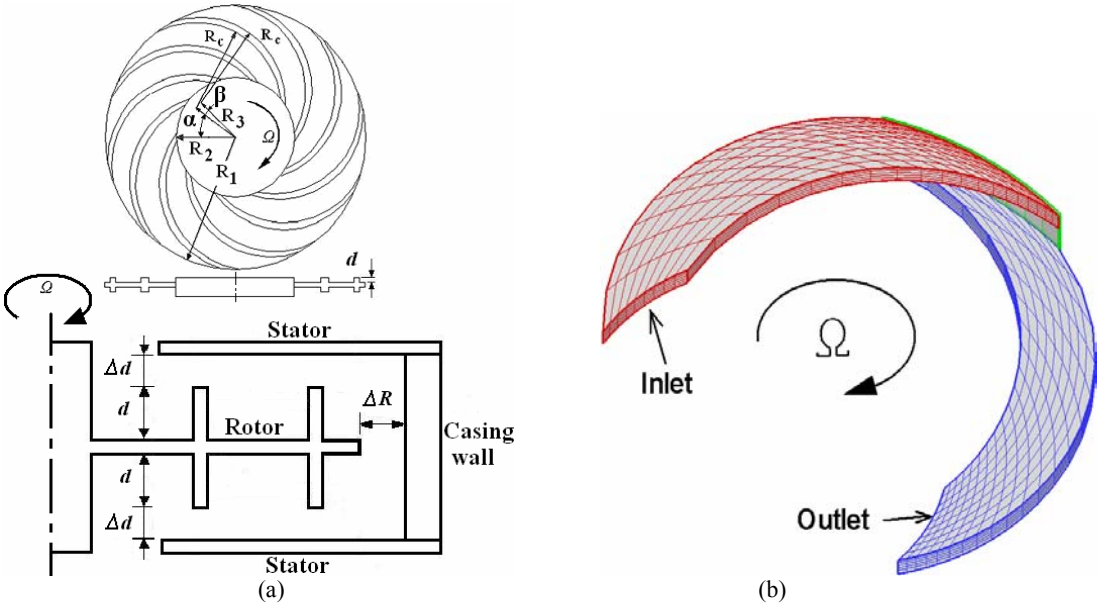

(a) (b)

FIGURE 1. Geometrical shape of a rotor: (a) rotor configuration and side view, (b) computational grid model for a single channel of DTDP.

TABLE 1. Geometrical dimensions of a rotor.

Name	Symbols	Dimensions
outer radius	R_1	86 mm
inner radius	R_2	39 mm
vertical clearance	$\triangle d$	0.1, 0.3, 0.5, 0.7, 0.9, 1.0 mm
radial clearance	$\triangle R$	1 mm
depth of channel	d	1, 1.5, 2, 2.5, 3, 3.5 mm
angle of inner channel wall	α	36°
angle of outer channel wall	β	8°
radius of channel	R_c	56mm
radius of channel center	R_3	32mm

A 3D body-fitted grid system of the rotor is shown in Fig. 1(b). The radial clearance $\triangle R$ between the rotor and casing wall is fixed in $\triangle R$ = 1 mm. For surface boundary conditions, the fully diffuse reflection assumption with the inelastic molecule-wall collision is employed for the interaction between the gas molecules and the surrounding surfaces of blades and walls by following the schemes of Heo and Hwang[11,12].

Results and Discussions

The DSMC simulations are carried out for a single stage (i.e., single rotor) DTDP with the computational grid illustrated in Fig. 1(b). The test gas is nitrogen at 273 K. In the present study, the Knusen number, $Kn = \lambda/(d+\triangle d)$, is based on the outlet pressure P_2 and the vertical length of a channel with clearance $d+\triangle d$ in Fig. 1(b). Computational results are obtained for the variation of the vertical clearance $\triangle d$ in the range of $0.1 \le \triangle d \le 1.0$ mm and of the variation depth of channel d in $1 \le d \le 3.5$ mm on the base of a fixed inlet and outlet pressure(P_1 = 30 Pa and P_2.= 140Pa) .

The pumping efficiency w is calculated by

$$w = \frac{N_{12} - N_{21}}{N_{inlet}}, \tag{1}$$

in which N_{12} (or N_{12}) is the number of molecules to be transmitted through the channel from the inlet (or outlet) to the outlet (or inlet), and N_{inlet} is the number of molecules coming from the inlet during sampling time[11,12].

The pumping speed S (l/s), and throughput Q($Pa{\cdot}l/s$) are calculated by

$$S = w \cdot A_1 \cdot \sqrt{8RT/\pi} \cdot K(s_1)/4.0, \tag{2}$$

$$Q = P_1 \cdot S, \tag{3}$$

in which A_1 is the area of the inlet, R is the gas constant, T is the absolute temperature

$$K(s_1) = \exp(-s_1^2) + \sqrt{\pi} s_1 \left[1.0 + erf(s_1)\right], \tag{4}$$

in which erf is the error function, s_1 ($= u_1/\sqrt{2RT}$) is the velocity ratio, and u_1 is the normal component of the bulk velocity of molecules crossing the inlet boundary, respectively[11,12].

The average pressure profiles along the pumping passage for six different vertical clearances are shown in Fig. 2, in which x is the local coordinate along the pumping channel and L is the total length along the centerline of the channel. The pressure change in the upper channel is very small in contrast with the dramatic change in the lower channel. The mark 'A' indicates the locations of radial clearance $\triangle R$.

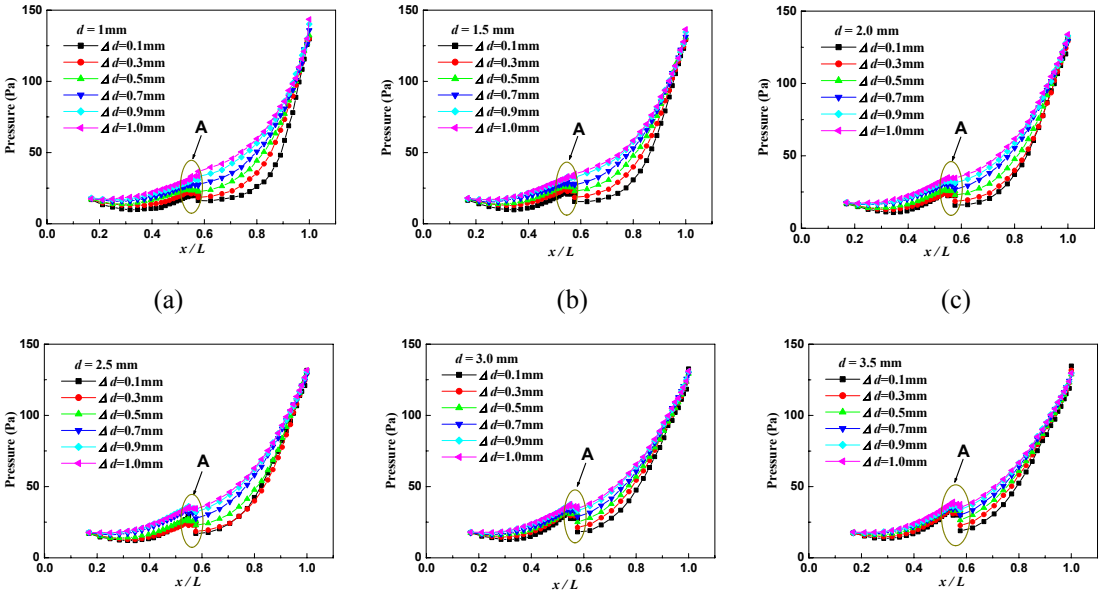

FIGURE 2. Pressure distribution along the pumping passage at P_2 = 140 Pa: (a) d = 1 mm, (b) d = 1.5 mm, (c) d = 2.0 mm, (d) d = 2.5 mm, (e) d = 3.0 mm and, (f) d = 3.5 mm.

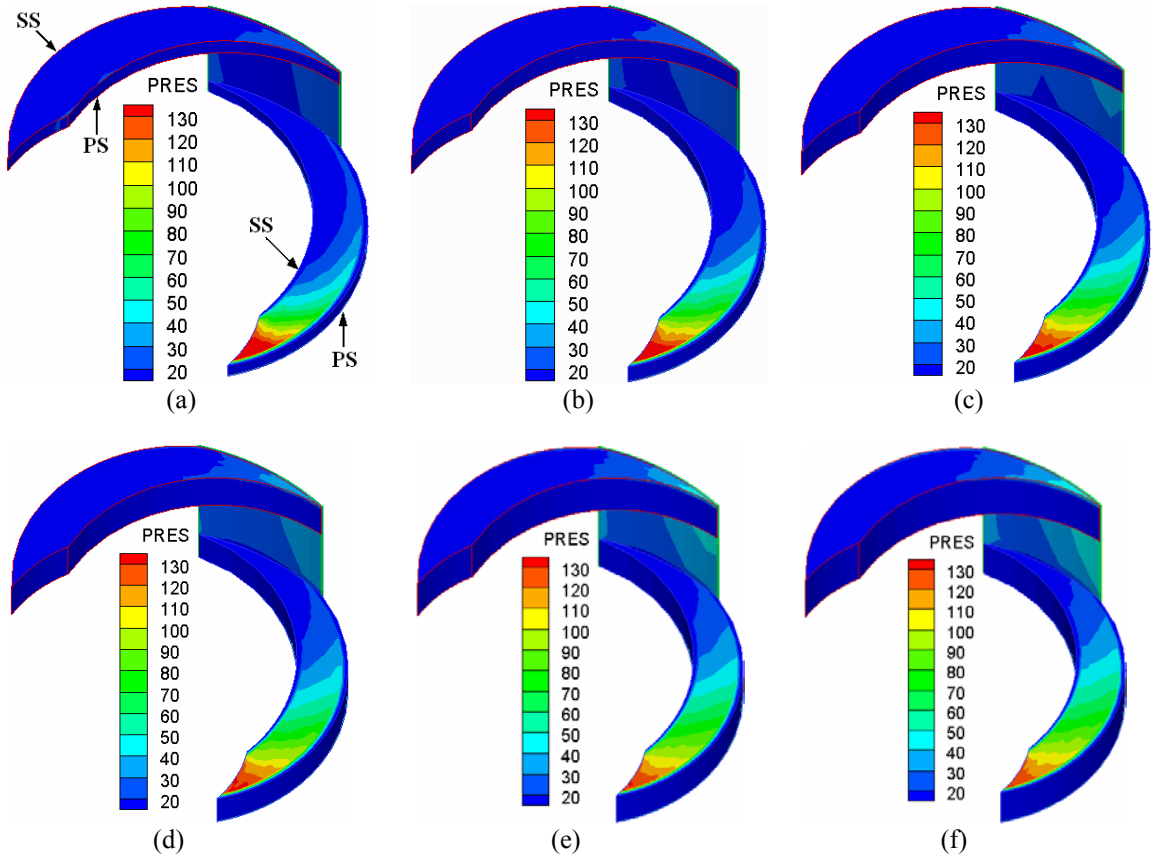

FIGURE 3. Pressure field for $\triangle d$ = 0.1 mm at and P_1 = 30 Pa and P_2 = 140 Pa (PRES unit: Pa): (a) d = 1 mm, (b) d = 1.5 mm, (c) d = 2.0 mm, (d) d = 2.5 mm, (e) d = 3.0 mm and, (f) d = 3.5 mm.

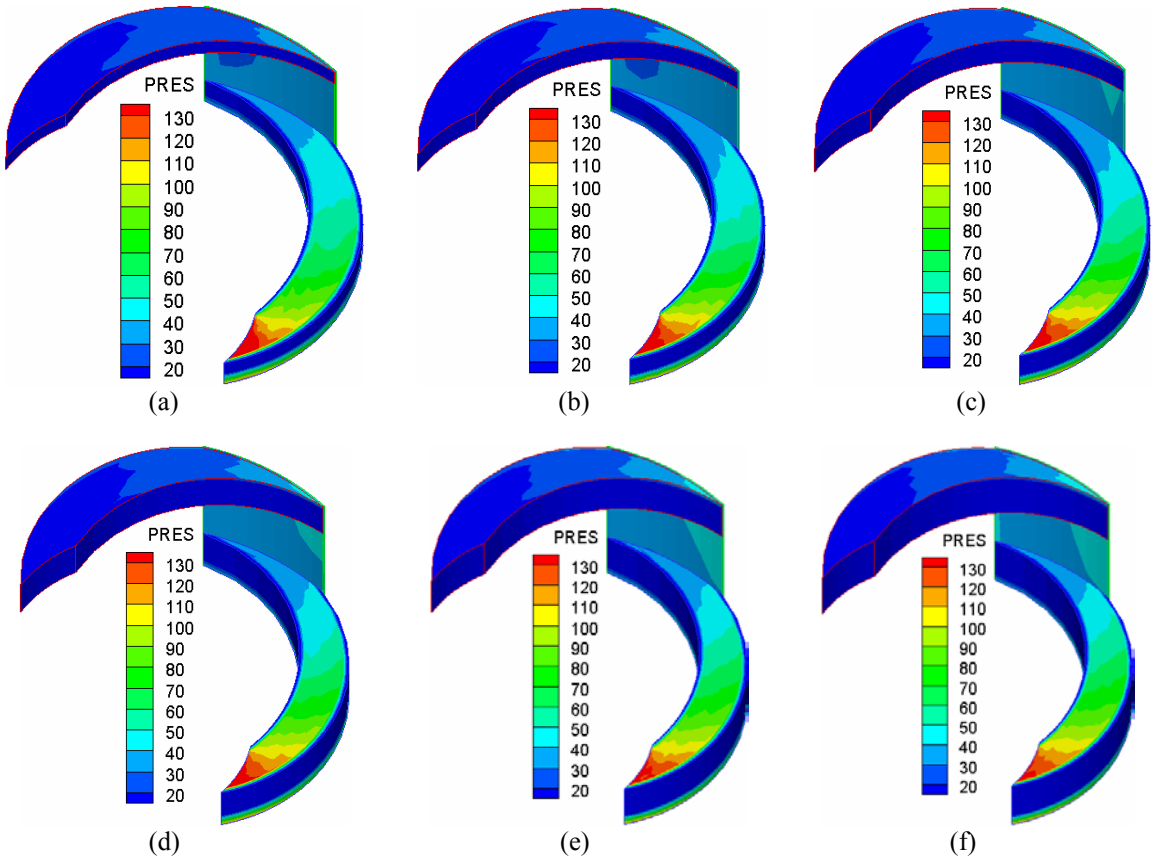

FIGURE 4. Pressure field for $\triangle d$ = 1 mm at and P_1 = 30 Pa and P_2 = 140 Pa (PRES unit: Pa): (a) d = 1 mm, (b) d = 1.5 mm, (c) d = 2.0 mm, (d) d = 2.5 mm, (e) d = 3.0 mm and, (f) d = 3.5 mm.

At the radial clearance, the pressure rise does not take place because of both the abrupt reduction in flow area and the high velocity. Most of the pressure rise occurs along the upper channel, as it can seen Figs. 2 and 4. The pressure rise for $\triangle d$ = 1 mm is the highest one along the upper channel, but the pressure gradient is the lowest near the outlet of lower channel, This is because the back flow rate through the vertical clearance becomes seriously higher as the vertical clearance $\triangle d$ increases.

The pressure contours of flow field, in Figs. 3 and 4, show that the pressure on the pressure surface (PS) of the spiral channel is higher than that on the suction surface (SS). In upper blades, the pressure is nearly constant from the inlet to the radial gap at $\triangle d$ = 0.1 mm, due to the smallest back flow rate of gas molecules. Also, it is found that the largest pressure gradient exists near the outlet of the lower channel. In general, the pressure contours shift toward the radial clearance, and they appear even in the upper channel, as the vertical clearance increases.

The pressure gradient of upper channel becomes larger as the depth of channel d increases. Also, it is found that relatively larger pressure drop occurs at the vertical clearance as d increases.

CONCLUSIONS

The gas flow in rotating channels of a DTDP in the molecular transition region is studied by using DSMC method for the variation of vertical clearance and depth of channel. Pressure density fields are obtained by the DSMC simulation. In the case of vertical clearance $\triangle d$ = 0.1 mm, the pressure rise of upper channels is the smallest one, but that of the lower channels is the largest near the outlet of pumping channels. Namely, the pressure rise of upper channels becomes relatively larger as the vertical clearance increases due to the flow leakage. It is hard for a DTDP to keep such small vertical clearance as $\triangle d$ = 0.1 mm, in practice. Therefore, it is recommended that the vertical clearance and channel depth be $\triangle d \leq 0.5$ mm, and $2.5 \leq d \leq 3.5$ mm, respectively.

ACKNOWLEDGMENTS

This work was supported by Korea Research Foundation Grant (KRF-2005-202-D00074)

.

REFERENCES

1. Hablanian, M. H., In *Vacuum Science and Technology: Pioneers of 20th Century,* AIP, New York, 1994.
2. Hablanian, M. H., *High Vacuum Technology (A Practice Guide),* Marcel Dekker, New York, 1990.
3. Heo, J. S. and Hwang, Y. K., *J. Vac. Sci. Technol. A* **18**, 1025-1034 (2000).
4. Hwang, Y. K. and Heo, J. S., *J. Vac. Sci. Technol. A* **19**, 662-672 (2001).
5. Liu, N. and Pang, S. J., *Vacuum*, 41, 2015-2017 (1990)
6. Shi, L., Wang, X. Z., Zhu, Y. and Pang, S. J., *J. Vac. Sci. Technol. A*, 11, 426-431 (1993).
7. Shi, L., Zhu, Y., Wang, X. Z. and Pang, S. J., *J. Vac. Sci. Technol. A*, 11, 704-710 (1993).
8. Sawada, T., *Vacuum*, 44, 689-692 (1993).
9. Sawada, T. and Nakamura, M., *Bull. JSME,* 29, 1770-1774 (1986).
10. Sawada, T. and Nakamura, M., *Vacuum* 41**,** 1833-1836 (1990).
11. Heo, J. S. and Hwang, Y. K., *J. Vac. Sci. Technol. A*. **20,** 1621-1631 (2002).
12. Heo, J. S. and Hwang, Y. K., *J. Vac. Sci. Technol. A*. **20**, 906-910 (2002).
13. Bird, G. A., *Molecular Gas Dynamics and the Direct Simulation of Gas Flows*, Clarendon, Oxford, 1994.
14. Borgnakke, C. and Larsen, P. S., *J. Comput. Phys.*, 18, 405-420 (1975).
15. Kwon, M. K. and Hwang, Y. K., " Performance Characteristics of a Disk-type Drag Pump in the Molecular Transition Region" in *24th International Symposium on Rarefied Gas Dynamics*, edited by Mario Capitelli, Conference Proceedings 762, American Institute of Physics, Melville, NY, 2004, pp. 236-241.
16 Kwon, M. K. and Hwang, Y. K., *Vacuum* 76, 63~71 (2004).